Dynamical arrest in dense short-ranged attractive colloids

2004 J. Phys.: Condens. Matter 16 S3791

(http://iopscience.iop.org/0953-8984/16/38/002)

INSTITUTE OF PHYSICS PUBLISHING JOURNAL OF PHYSICS: CONDENSED MATTER

J. Phys.: Condens. Matter **16** (2004) S3791–S3806 PII: S0953-8984(04)78466-0

Dynamical arrest in dense short-ranged attractive colloids

G Foffi[1], F Sciortino[1,2], E Zaccarelli[1,2] and P Tartaglia[1,3]

[1] Dipartimento di Fisica and INFM, Università di Roma La Sapienza, I-00185 Rome, Italy
[2] SOFT, Istituto Nazionale per la Fisica della Materia, Complex Dynamics in Structured Systems Centre, Rome, Italy
[3] SMC, Istituto Nazionale per la Fisica della Materia, Statistical Mechanics and Complexity Centre, Rome, Italy

Received 26 March 2004, in final form 28 July 2004
Published 10 September 2004
Online at stacks.iop.org/JPhysCM/16/S3791
doi:10.1088/0953-8984/16/38/002

Abstract

We study thermodynamic and dynamic properties of model colloidal systems interacting with a hard core repulsion and a short-range attraction, and provide an overall picture of their phase diagrams which shows a very rich phenomenology. We focus on the slow dynamic properties of this model, investigating in detail the glass transition lines (both repulsive and attractive), the glass–glass transitions and the location of the higher order singularities. We discuss the relative location of the glass lines and of the metastable liquid–gas binodal, an issue relevant for the understanding of low density arrested states of matter.

1. Introduction

Colloidal systems have a wide range of applicability in various fields. For basic science research, they constitute a very appealing model system for studying particle interactions at a mesoscopic scale. This is essentially due to the fact that the interparticle forces can be tailored to a great extent with fairly simple chemical methods. Another important reason is related to the size of the colloidal particles which is much larger than that of particles in a molecular fluid, opening up significantly the range of values of physically relevant parameters. For example, novel phenomena arise when the range of particle–particle interaction becomes significantly smaller than the size of the particle and when the system is composed of colloidal particles with significantly different size or mobility. Recently, new interest has arisen in colloidal systems where, besides the usual short-ranged repulsive interaction, attractive forces play a significant role [1]. The latter can be achieved in real systems in many different ways, for example by means of depletion forces, by dissolving polymers in a solution of colloidal particles, or grafting polymers on the surfaces of colloids. The effect of attractive forces of very short range on thermodynamics has been studied in the past: a new relevant phenomenon

appears, i.e. the disappearance of the liquid phase in the phase diagram of the system [2]. This effect can be easily observed in colloidal systems where the size of the particle can be made much larger than the range of the attractive forces. From the theoretical point of view the study of short-ranged attractive forces was pioneered by Baxter [3], with his celebrated attractive hard spheres (AHS) model, for which he provided an exact solution in a special case, and which is still one of the basic simple models in the physics of colloids. A very accurate numerical simulation of the AHS model was performed recently and compared with the Baxter solution [4].

In the last few years new interesting dynamic phenomena have been predicted theoretically in the case of dense attractive colloids by means of the application of the prescription of the mode-coupling theory (MCT) for supercooled liquids [5] to short-range attractive colloids [6, 7]. Most of these phenomena have been related to the existence of higher order kinetic singularities of the glass transition that were hypothesized from MCT but never convincingly observed in real systems. Surprisingly, in a relatively short time various theoretical predictions have been proven to be valid in many different colloidal systems and with diverse experimental techniques [8–14]. Numerical simulations have also been widely employed to test the MCT predictions and the details of the theory [15–23]. The formation of a glass at low volume fractions could have rather important consequences in many different ways. Just to give some examples, it was speculated that the formation of a gel at low volume fraction of the dispersed phase might be a manifestation of the structural arrest associated with the glass transition. Another interesting aspect of such phenomena, the formation of an amorphous state close to an equilibrium phase transition, might be related to the problem of protein crystallization.

In the next section we will summarize the predictions of MCT for the general case of a repulsive potential followed by a short-ranged attractive interaction, while the following section deals with numerical simulations of square well systems. We will conclude with an outlook on possible developments in the study of such systems.

2. Predictions of MCT

Pure hard sphere systems can be easily realized using colloidal systems and have been extensively studied in concentrated samples through accurate dynamic light scattering experiments [24]. One of the most striking successes of the MCT is the very good description that it gives of the supercooled glass transition; in particular, the most striking feature of dynamical light scattering, i.e. the two-step relaxation processes (called β- and α-relaxation at short and long times respectively), have been carefully studied and identified. Experiments have also approached very closely the non-ergodicity transition which signals the formation of a glass phase; the corresponding non-ergodicity parameter f_q, i.e. the long-time limit of the density time–correlation function, has also been measured as a function of the momentum transfer q.

The typical behaviour of hard sphere systems is not always present in colloidal systems; there are many cases where deviations from MCT predictions have been observed [25, 26]. For example, in a solution of polymer coated colloidal particles [25] a typical two-step decay was observed, but, contrary to the usual situation, the non-ergodicity factor reaches rather unexpected high values. Moreover, a structural arrest line, different from that of conventional percolation, is observed and extends inside the metastable binodal line. In a system made up of microgel particles, a peculiar logarithmic decay in time of the density correlators is observed [26], completely absent for pure hard sphere systems and not predicted by the conventional theory.

The first application of MCT to a case of a repulsive potential followed by an attractive tail was made with reference to the Baxter model [6, 7], where the range of the attraction Δ vanishes while its depth $-u_0$ becomes very large, in such a way that in the limit the quantity $\tau = \exp[-u_0/k_BT]/12\epsilon$ tends to a constant value. $\epsilon = \Delta/(\sigma + \Delta)$ is a dimensionless width parameter, with σ the hard core diameter. Provided that an appropriate momentum cut-off is introduced [27], peculiar effects set in, leading to new relevant phenomena. We will list the most important ones in what follows, and study some of them in detail in the following paragraphs.

For large volume fractions ϕ and high temperatures T, the system is dominated by the well-known cage effect since a particle surrounded by the crowd of other particles can only move if there is a simultaneous motion of the surrounding ones, the 'cage'. For $\phi \simeq 0.516$, MCT predicts a structural arrest [28], with an offset compared to the experimentally observed case of the order of 10–15%, since in the latter case $\phi = 0.58$. This is the glass transition observed a long time ago in colloidal systems that can be considered as hard sphere systems. As temperature is lowered, the transition line moves to higher values of ϕ. The behaviour of the non-ergodicity factor as a function of q has the typical hard sphere aspect. Quite unexpectedly, a second structural arrest line appears that extends from low to high volume fractions, meeting the previously found repulsive glass line and continuing inside the region where the system forms an amorphous glass. The latter feature produces a line separating two different types of glass, i.e. it produces a glass–glass transition that we will describe later. This phenomenon is clearly related to the attractive tail of the potential and gives rise to a glass transition line which was called the attractive or gel line. Similar behaviour was observed when using an attractive Yukawa tail in the interparticle potential [7]. The physical interpretation of the formation of an attractive glass has been related to the fact that the free motion of the particles is not possible any longer due to the adhesiveness of the potential. When the particles come very close to one another, they tend to stick together, thus creating an obstacle to the motion even at low volume fractions. This interpretation can be made more quantitative by considering the localization length of the glassy systems, which can be derived from a study of the mean squared displacement of the colloidal particles. In the case of the repulsive glass it is of the order of 0.1σ while for the attractive glass it is given by the attractive potential range Δ. One of the distinguishing features of this new type of glass transition is the overall shape of the non-ergodicity factor as a function of q. It has a typical complex structure which is quite different from the repulsive case and with reaches much higher values, as we will discuss in the next section. These predictions of MCT are quite robust and are observed in various model systems with different kinds of attractive tails—namely, besides Baxter and Yukawa potentials, also the case of the simple square well potential [15] and the Asakura–Oosawa depletion interaction [16, 21]. Finally, we note that different types of closure of the Ornstein–Zernike equation have been employed in order to derive the structure factor S_q needed as an input to the MCT equations, without relevant changes in the predictions reported above.

2.1. The repulsive and attractive glass lines for square well systems

We will now give detailed results obtained for a system that we used as prototype for attractive colloids, i.e. the short-range square well (SW) system, where the potential is given by

$$V(r) = \begin{cases} \infty & r < \sigma \\ -u_0 & \sigma < r < \sigma + \Delta \\ 0 & r > \sigma + \Delta \end{cases} \tag{1}$$

where $\epsilon = \Delta/(\sigma + \Delta)$ typically has the value 0.03, but ranges between 0.001 and 0.09 in the various cases that we studied. We choose $k_B = 1$ and the depth of the potential $u_0 = 1$.

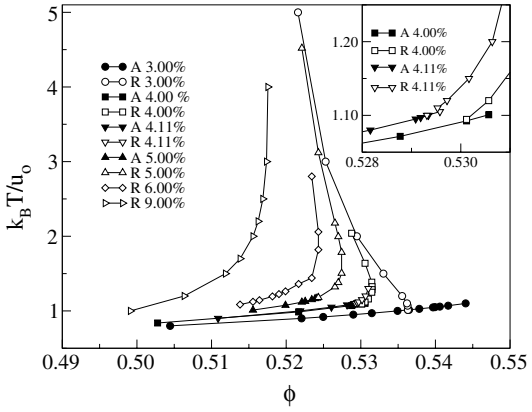

Figure 1. The phase diagram of the SW system for various widths. R and A indicate repulsive and attractive liquid–glass curves respectively. The inset details how the glass–glass transition curves vanish for a well width around 4.11%. Redrawn from [15].

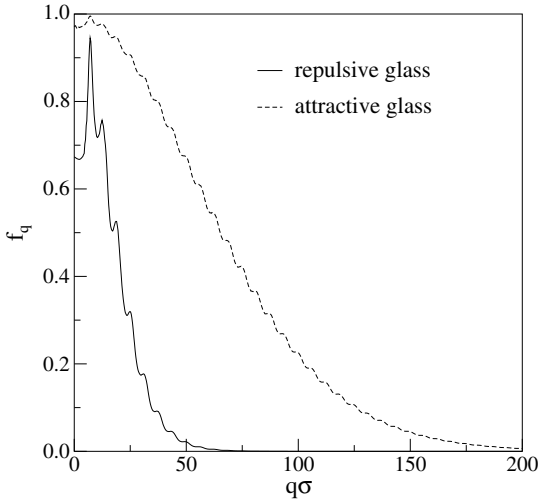

Figure 2. The non-ergodicity factors of the SW system for $\phi = 0.54$ and $T = 1.5$ for the repulsive and $T = 1.0$ for the attractive case.

In figure 1 we show a region of the phase diagram in the plane $(\phi, k_B T/u_0)$ for a SW system characterized by the width parameter $\epsilon = 0.03$–0.09 and $u_0 = 1$, the unit of energy. The attractive and repulsive lines start to appear when $\epsilon \sim 0.04$ and are most clearly visible for $\epsilon = 0.03$. The non-ergodicity factors f_q for the two types of glass are depicted in figure 2 which clearly shows that the attractive non-ergodicity factors are always higher than the corresponding repulsive ones.

When the attractive potential width is small enough, a region of the phase diagram appears which contains a pocket of liquid states, a result of the adhesive interactions. In other words, the liquid is stabilized with respect to the formation of a glass and forms a re-entrant region, starting from which one can get an arrested glassy state both on lowering and on raising the temperature. In this case the attractive glass line terminates at a point inside the glassy region, which in the language of MCT is a higher order bifurcation point related to the solutions of the asymptotic MCT equations. That is, it is an A_3 point as opposed to the normal A_2 point of

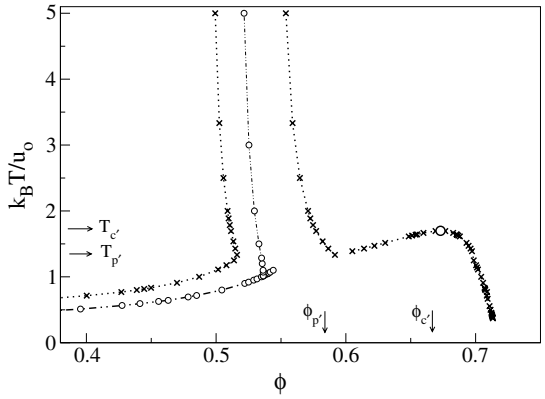

Figure 3. The phase diagram for the SW model for $\epsilon = 0.03$. The crosses represent the solid–fluid phase coexistence and the set of open circles is the glass line. Note the solid–solid coexistence on the high density side of the phase diagram: its critical point is labelled with a filled circle. The position of the liquid–solid–solid triple point is also displayed, $(\phi_{p'}, T_{p'})$.

the repulsive glass. The portion of the attractive glass line that is inside the amorphous region separates two different glass types, and it is a glass–glass transition boundary. A discontinuity of the non-ergodicity factor f_q is present along the line and disappears at the A_3 point. The relevant aspect of the higher order singularity in the framework of MCT is the fact that the density–time correlation functions have a logarithmic decay over a long time interval. This corresponds to a limiting behaviour of the typical (two-step) power law behaviour close to the non-ergodicity plateau when the exponents tend to vanish. This happens when the system is in a supercooled state but deep in the re-entrant region, where the effect of the nearby higher order singularity is important. We will return to this point when comparing with the numerical simulation results.

2.2. The equilibrium phase transition diagram

It is interesting to consider the interplay between the ideal glass line calculated within MCT and the thermodynamic phase boundary. This has been studied in detail for a Yukawa model potential in [17] and it has been related to the problem of the protein crystallization [29]. For the Yukawa model, it has been possible to relate the overall structure of the phase diagram and the glass transition line to the general one proposed for protein crystallization [30]. Indeed when the range of the potential becomes short the thermodynamics shows special features that have been well established in the last decade. The disappearance of the liquid–liquid phase boundary and the appearance of a isostructural phase coexistence, typical in this class of potentials, have been established either in experiments or simulations [2].

In figure 3, we present the ideal glass transition line for the square well system with $\epsilon = 0.03$ plotted together with the fluid–solid–liquid coexistence line. The latter line has been calculated with thermodynamic perturbations as was done originally by Gast *et al* [31]. The underlying crystal structure is assumed to be fcc. It is interesting to note that the ideal glass transition line lies within the fluid–solid coexistence line and that its shape is very close to the shape of the phase boundary lines. At this value of the range of attraction the glass–glass line extends into the glass region at high packing fraction, separating the hard core from the attractive glass. On increasing the range, the line shrinks and eventually vanishes. Similarly the isostructural phase coexistence disappears when the range is above a certain value. Moreover, the origins of the two crystal structures are related again to attraction and repulsion.

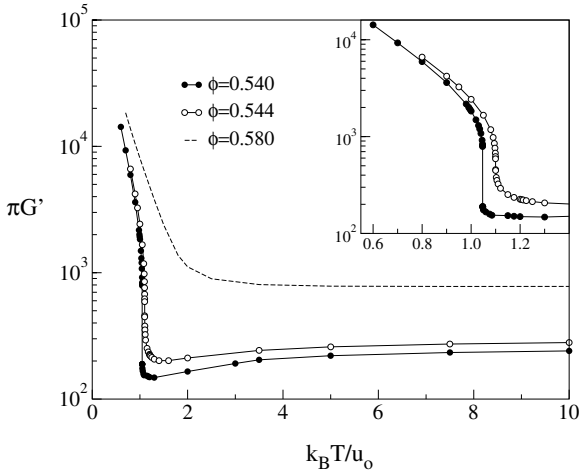

Figure 4. The static shear moduli on crossing the glass–glass transition line for $\epsilon = 0.03$ ($\phi = 0.540$) and close to the A_3 bifurcation point ($\phi = 0.544$) and at a density where the repulsive and attractive glasses have become indistinguishable ($\phi = 0.580$). The inset shows an enlarged view of the glass–glass transition region. Redrawn from [32].

2.3. The shear moduli

Another interesting way of characterizing the glass–glass transition can be obtained using calculations of the shear viscosity and the elastic shear modulus which are capable of detecting the difference between a repulsive and an attractive glass. The two quantities can be measured in real systems and such measurements can provide good insight into the glass transition phenomenon and its relation with MCT. The complex shear viscosity $\eta^*(\phi, T, \omega)$ can be calculated in terms of the normalized time correlation function of the density fluctuations $\phi_k(t)$ [33, 34]:

$$\eta^*(\phi, T, \omega) = \frac{k_B T}{60\pi^2}\int_0^\infty \mathrm{d}t\, \mathrm{e}^{\mathrm{i}\omega t}\int_0^\infty \mathrm{d}k\, k^4\left[\frac{\mathrm{d}\ln S_k}{\mathrm{d}k}\phi_k(t)\right]^2 \tag{2}$$

and is related to the complex shear modulus $G^*(\phi, T, \omega)$ by

$$G^*(\phi, T, \omega) = \mathrm{i}\omega\eta^*(\phi, T, \omega). \tag{3}$$

We note that this formula, since it depends on the square of the correlation function, is different in structure from that used by Weitz and co-workers, where the stress-relaxation function is linearly related to the density correlation function [35]. All the quantities in the equations (2) and (3) can be easily evaluated for the present system by performing the integrals with standard numerical integration. Before discussing the results, we should stress that the previous equations are used, within the MCT, in the glassy region where ageing phenomena, which are very important in real systems, are ignored by the theory. The considerations that we will develop in the following, concerning ageing from the re-entrant region and the study of the glass–glass line, apply to this situation too.

In figure 4 we report the behaviour of the shear modulus G' upon crossing the attractive glass line in the glassy region. In figure 4 the static shear modulus, i.e. the zero-frequency limit of equation (3), has been represented for three different packing fractions ($\phi = 0.540$, 0.544 and 0.580) as a function of temperature. These three cases correspond to crossing the glass–glass line, crossing the A_3 point and a density where the repulsive and attractive glasses

have become indistinguishable. In the first case it is clearly possible to distinguish between the two glasses. For low temperatures there is strong dependence of the elastic viscosity on temperature; in particular, the system becomes more and more rigid on decreasing the temperature. When the system crosses the glass–glass transition there is a discontinuity in the elastic response which clearly indicates that the structure is changed. On increasing the temperature further the elastic behaviour does not change so much any longer and for large temperatures the system behaves like a hard sphere suspension. In this case the glass originates from the cage effect and consequently the particles are forced to move inside a fixed volume that does not change with temperature. We have noted that the difference in the shear modulus as the A_3 point is approached is described by a power law, and it is also possible to show that in this regime the differences in mechanical properties of the two systems are due to the different shapes of the non-ergodicity parameter f_q, and hence the long-time residual motions in the gel, and not to the contribution of the equilibrium structure factor [32].

3. The numerical simulation of the SW system

In order to check the predictions of the MCT we have undertaken an accurate molecular dynamics (MD) study of the various aspects of the behaviour of a very short-ranged SW system where many new features of the structural arrest tend to be manifested. The system that we study is a 50%–50% binary mixture of $N = 700$ (and in many cases 2000) hard spheres of unit mass m, with diameters σ_A and σ_B and ratio $\sigma_A/\sigma_B = 1.2$, interacting via the interparticle potential given by

$$V_{ij}(r) = \begin{cases} \infty & r_{ij} < \sigma_{ij} \\ -u_0 & \sigma_{ij} < r_{ij} < \sigma_{ij} + \Delta_{ij} \\ 0 & r_{ij} > \sigma_{ij} + \Delta_{ij} \end{cases} \tag{4}$$

where $\sigma_{ij} = (\sigma_i + \sigma_j)/2$, $i, j = \mathrm{A}, \mathrm{B}$ and Δ_{ij} has been chosen in such a way that $\epsilon_{ij} = \Delta_{ij}/(d_{ij} + \Delta_{ij})$ typically has the value 0.03, but ranging between 0.001 and 0.09 in the various cases that we studied. As for the one-component case, $T = 1$ corresponds to a thermal energy equal to the attractive well depth. The diameter of the small species is chosen as the unit of length, i.e. $\sigma_B = 1$. Density is parametrized in terms of the packing fraction $\phi = (\rho_A d_A^3 + \rho_B d_B^3)\pi/6$, where $\rho_i = N_i/L^3$, L being the box size and N_i the number of particles for each species. Time is measured in units of $\sigma_B(m/u_0)^{1/2}$. A standard event-driven MD algorithm has been implemented for particles interacting with SW potentials. Between collisions, particles move along straight lines with constant velocities. When the distance between the particles becomes equal to the distance where $V(r)$ has a discontinuity, the velocities of the interacting particles instantaneously change. The algorithm calculates the shortest collision time in the system and propagates the trajectory from one collision to the next one. Calculations of the next collision time are optimized by dividing the system into small subsystems, so only times of collisions between particles in the neighbouring subsystems are computed. The small asymmetry in the diameters of the two components of the mixture is sufficient to prevent crystallization at high values of ϕ.

3.1. The repulsive and attractive glass lines

The glass lines are determined by measuring the mean squared displacement of the colloidal particles and deriving from it the diffusion coefficient D using the Einstein relation

$$D = \lim_{t\to\infty} \frac{\langle |r(t) - r(0)|^2 \rangle}{6t}. \tag{5}$$

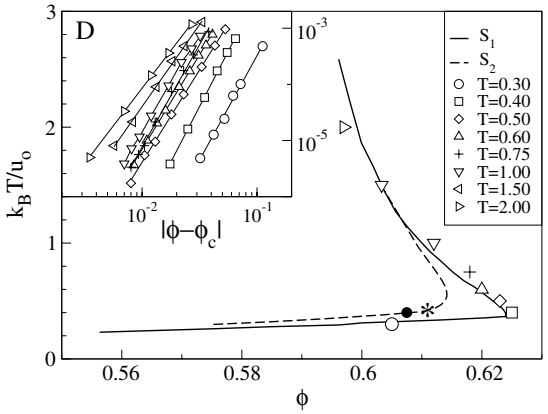

Figure 5. The phase diagram of the SW system with $\epsilon = 0.03$ (labelled S_1) obtained by numerical simulation. Also, the case $\epsilon = 0.0411$ (labelled S_2), obtained by using the transformation in equation (6), is shown. The inset shows the power laws associated with the diffusivity.

These values are then scaled by a normalization factor $D_0 = \sigma\sqrt{T/m}$ in order to take into account the temperature dependence of the microscopic time. According to MCT, on approaching structural arrest D tends to vanish following a power law, a behaviour well verified in the case of our simulation as shown in the inset of figure 5. In this way we can trace the locus of $D/D_0 = 0$ in the (ϕ, T) phase diagram. As already discussed earlier, it is well known that MCT produces a displacement of the order of 10–15% from the observed experimental glass transition, so in order to compare theory and numerical simulation we need to apply a bilinear coordinate transformation

$$\begin{aligned} \phi_{\text{sim}} &\to 1.897\phi_{\text{MCT}} - 0.3922 \\ T_{\text{sim}} &\to 0.5882T_{\text{MCT}} - 0.225 \end{aligned} \tag{6}$$

which allows us to superimpose the MCT result with the simulation data, in the region of T and ϕ studied. Figure 5 compares the glass points extrapolated from the diffusivity with the results of transformation (6). An added result is the possibility of locating the A_4 point, as well as the terminal value of the line of A_3 points which according to MCT is at $\phi = 0.64$ and $T = 0.41$. One of the following subsections will deal with the behaviour of the density correlators at A_4, the only higher order point accessible from the supercooled liquid side.

At this point we should stress that the simulation confirms the MCT predictions only on the high volume fraction side of the phase diagram for $\phi > 0.6$. As the volume fraction ϕ decreases, the attractive glass line temperature slightly decreases and the line is expected to move almost parallel to the ϕ axis. Within the SW model, it is important to locate this line in the phase diagram and to frame its position with respect to the metastable liquid–gas binodal. Indeed, if the attractive glass line is above the critical liquid–gas point, an arrested state can be approached from equilibrium. In the other case, where the attractive glass line ends on the high density side of the binodal, low density arrested states can be generated only via a phase separation mechanism. For the case of $\epsilon = 0.03$, the intersection between the attractive glass line and the binodal was shown to take place at rather high packing fractions [36]. In order to check the well width dependence of the crossing point, we report in figure 6 preliminary results concerning a binary SW system, with $\epsilon = 0.001$, using 2000 colloidal particles and the same parameters as we employed before. Using these parameters we can, to a first approximation, use the known location of the binodal line of the Baxter model, which has been recently carefully

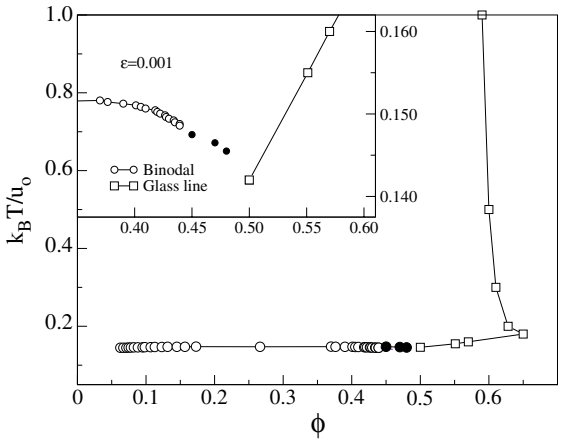

Figure 6. The crossing of the binodal and the glass lines for the case $\epsilon = 0.001$. The binodal line being very flat, the crossing of the two lines is shown in the inset. The solid points are binodal points evaluated from the simulation.

studied over a large range of values of ϕ [4]. The attractive glass line, calculated again by extrapolating the vanishing diffusivity, meets the binodal at $\phi = 0.45$ and $k_B T/u_0 = 0.14$, not much below the critical point at $k_B T_c/u_0 = 0.151$, as estimated, via the second virial coefficient mapping, from the simulation of the AHS system [4]. It is worth noting at this point that a quench from the one-phase to the two-phase region, below the temperature of crossing of the glass and spinodal lines, would produce a separation of the system into two phases: a 'gas'-like and an attractive glass one. It is likely that in order to have the binodal line below the glass one, it is necessary to shrink the range of the attractive interaction even further. Note that the point where the glass line meets the binodal is only less than 3% away from the critical point, suggesting that with a much narrower potential well (unphysical with present day colloidal systems) it might be possible to extend the attractive glass line above the critical temperature.

3.2. Ageing from the re-entrant region

As we have discussed, an interesting possibility related to the re-entrant shape of the glass transition line is the possibility of generating states with long relaxation time both by decreasing and by increasing the strength of the attraction, hence accessing either the repulsive or the attractive glass regions. This phenomenology suggests the possibility of characterizing short-ranged attractive systems also by their non-equilibrium dynamics. It is well established in experiments and simulation [37, 38] that if a system is quenched in the region where the relaxation time is much longer than the observation time, ageing starts to play an important role. The system, forced into an out-of-equilibrium situation, does not obey time translation invariance; consequently the relevant observable will depend strongly on the time elapsed from the quench out of equilibrium, the so-called waiting time t_w. In particular, the two-time correlation function (such as the mean square displacement or the intermediate scattering function) will depend not only on the absolute time t but also on the waiting time t_w. For a binary mixture of Lennard-Jones particles, Kob and Barrat showed that quenches below the mode-coupling glass transition temperature produce a relaxation time that grows with the waiting time [37]. For the short-ranged attractive SW system we find the unique possibility

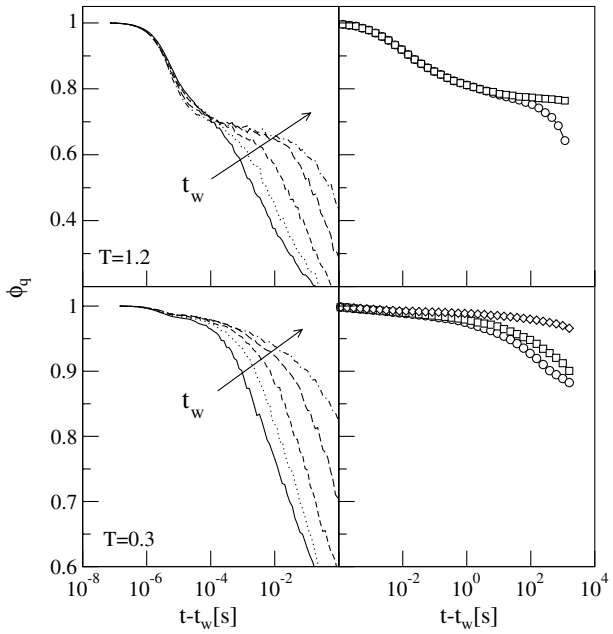

Figure 7. Left panel: total density–density correlation functions for $q\sigma_B = 2.93$ at different waiting times for $T_f = 1.2$ and 0.3. From left to right, longer and longer relaxation time, $t_w = 3.67 \times 10^{-4}, 3.67 \times 10^{-3}, 3.67 \times 10^{-2}, 3.67 \times 10^{-1}, 3.67 \times 10^{0}$ s. The unit of time $\sigma(m/u_0)^{1/2}$ used in the simulations has been converted to seconds using $m = 4.1086 \times 10^{-17}$ kg, $\sigma_A = 2.02 \times 10^{-7}$ m and $u_0/k_BT = 1/1.2$ with T evaluated at ambient temperature, consistent with the experimental conditions. With this choice, $\sigma(m/u_0)^{1/2} = 3.67 \times 10^{-5}$ s. Right panel: experimental data reproduced from [13] for quenches in the repulsive and the attractive (bottom) glass.

of forcing the system out of equilibrium by quenching it either at low or at high temperature starting from an equilibrated point within the re-entrance. We tackled this possibility by means of numerical simulations [39].

Because the system is out of equilibrium, averages cannot be performed over time but must instead be done over independent initial configurations. Hence, we prepared 60 independent configurations, equilibrated at the initial temperature $k_BT_i/u_0 = 0.6$ and at a density of $\phi = 0.608$. This state point can still be properly equilibrated in MD and it lies in the re-entrant region of the glass line. We quenched these independent configurations to the desired final temperatures, and then followed the evolution over time at constant temperature. The characteristic time of the thermostat has been chosen to be much smaller than the structural relaxation time and such that the system may equilibrate within one time unit. Each of the 60 independent configurations has been quenched to $k_BT_f/u_0 = 1.2$, i.e. in the repulsive glass, and to $k_BT_f/u_0 = 0.3$, i.e. in the attractive glass, and run up to $t_f = 2 \times 10^5$. The system is the usual binary mixture of 700 particles with SW interactions.

In figure 7 (right panel) we present the results for the density–density correlation function. The averages are performed over the 60 initial configurations and no distinction has been made between the two species. As for other ageing systems, the structural relaxation time grows with t_w. However, the two quenches present completely different dynamics, which are characteristic of the different origins of the two underlying glasses. In the left panel of figure 7, we present experimental data for colloidal particles produced by Pham *et al* [13]

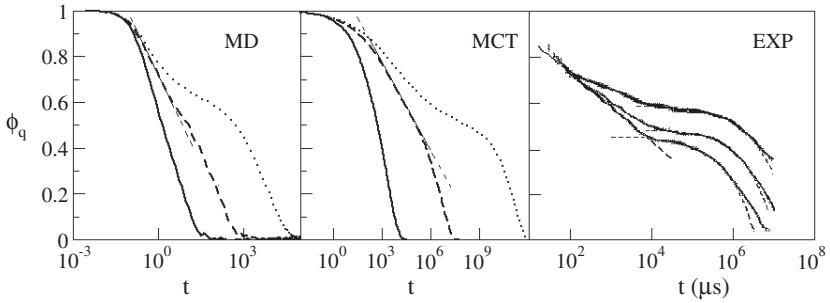

Figure 8. Comparison of the density correlators obtained by means of MD, MCT and experimentally ('EXP'; see the text for the details). The logarithmic behaviour on approaching the position of the non-ergodicity plateau is feature common to the three cases, as shown by the straight dashed lines.

for two quenches in the repulsive and attractive glasses. Our results are in good qualitative agreement with experimental data.

3.3. The higher order singularities A_3 and A_4

The direct study of the higher order singularity of type A_3 is complicated by its being buried in the glass region. However, it is predicted by MCT that even in the liquid region the singularity will display its effects. In particular, state points in the phase diagram in the re-entrant region that are relatively close to A_3 will be characterized by a logarithmic behaviour of the density–time correlation functions, due to the vicinity of this point.

In figure 8 we display density correlators obtained in different ways in order to emphasize their similarity. Starting from the left we shows three correlators for the usual binary SW system at $\phi = 0.58$, 0.60 and 0.61 for the case $\epsilon = 0.03$ in the re-entrant region for $T = 0.75$. In the middle panel the same functions as obtained using the MCT calculations are shown. Finally, in the last panel we report a sample of the measurements performed on a tri-block co-polymer system (pluronic L64) at various temperatures and fixed concentration of the polymers [8]. All three panels show qualitatively similar behaviours, typical of a supercooled liquid in the re-entrant region, i.e. a logarithmic decay in time after the initial transient, followed by a power law behaviour which typically follows the von Schweidler power law in time. From the point of view of numerical simulation a similar anomalous behaviour is observed in the mean squared displacements of the colloidal particles which show a sub-diffusive behaviour.

MCT predicts the existence for our model of a higher order singularity of type A_4, where the liquid, the repulsive glass and the attractive glass solutions merge into a single point. This is realized for a particular point in the control parameter space, namely (ϕ^*, T^*, Δ^*). The theory also gives detailed predictions for the behaviour of dynamical observables, i.e. logarithmic decay for the density autocorrelation functions and sub-diffusive behaviour for the mean squared displacement, approaching the A_4 point [40]. To test these predictions, we need to locate the higher order singularity for our model. In this way, we can approach it *from the liquid side* and analyse the control parameter dependence (in particular, the Δ dependence) of the dynamical observables, determining whether the A_4 point is really there. To realize this, we adopted the following procedure.

- We solved the long-time limit MCT equations for our particular binary mixture in order to locate the ideal glass line. As inputs, we used the partial static structure factors

calculated within the Percus–Yevick approximation for the same mixture, obtained by numerically solving the Ornstein–Zernike equation on a grid of 20 000 wavevectors, with mesh 0.314 1593. The binary MCT equations are then solved on a grid of 2000 wavevectors with the same mesh.

- We evaluated the diffusion coefficients from simulations, as the long-time limit of the mean squared displacement, using Einstein's relation. This is done in the liquid region for various temperatures, up to the order of magnitude 10^{-5} in diffusivity. For each isotherm we fit our results with the power law $D \sim (\phi - \phi_g(T))^\gamma$, extracting the fit parameters $\phi_g(T)$ and γ, which are respectively the glass transition packing fraction (at which the diffusion coefficient would vanish) at temperature T and a characteristic exponent which, according to MCT predictions, should grow near a higher order singularity.
- We performed the bilinear transformation, already announced in (6), in the control parameter space (ϕ, T), to superimpose MCT results for the ideal glass line with the extrapolated results from the simulations, following an idea proposed by Sperl [40], as discussed before.

With this procedure, assuming that the bilinear transformation does not depend on Δ close to the A_4 point, the A_4 point has been located at $\epsilon^* = 0.0411$, and marked with a star symbol in figure 5. On the basis of this mapping, we have performed MD simulations for the 4.11% case, and studied, for a single state point close to the A_4 singularity, marked as a full black circle in figure 5, the variation of the MSD and density correlation functions with respect to the 3% case. These functions were analysed and an extremely good agreement with MCT predictions was found, supporting the mapping procedure, and, most importantly, giving a clear confirmation of the existence of the A_4 singularity [22].

As stated above, the density correlation functions near the A_4 singularity are predicted to decay, to lowest order within MCT [40], as follows:

$$\phi_q(t) = f_q - h_q \left[B^{(1)} \ln(t/\tau) + B_q^{(2)} \ln^2(t/\tau) \right] \tag{7}$$

where f_q is the value of the non-ergodicity parameter of the singularity, τ is a timescale that grows approaching the singularity and $h_q B^{(1)}$, $h_q B_q^{(2)}$ are the amplitudes of the logarithmic terms. Thus, in general, for any wavevector, the shape of the density correlators is not purely logarithmic, and there are higher order corrections. However, the coefficient of such a correction depends on the wavevector, through $B_q^{(2)}$. Thus, one can determine a particular q^*, which is state point dependent, for which $B_{q^*}^{(2)} = 0$. At this length scale, the decay is purely logarithmic. A confirmation of this behaviour is found with simulations, and illustrated in figure 9. Here, we show the density correlation function for the state point $\phi = 0.6075$ and $T = 0.4$, for S_1 and S_2. Each correlator refers to the particular q^* relating to each of the two state points, respectively $q_1^* = 23.5/\sigma_{BB}$ for S_1 and $q_2^* = 16.8/\sigma_{BB}$ for S_2. This value is significantly smaller than the nearest-neighbour length, signalling the importance of the attractive range in the system. A detailed study of the wavevector dependence of the density correlators had already been performed in [22], showing an overall very good agreement with MCT predictions. Here, we want to stress that, varying Δ, we are approaching the A_4 singularity from the liquid side, and the range of validity over time of equation (7) grows by more than one order of magnitude (see the vertical lines in the figure) between the two values studied numerically. This strongly supports the notion of the existence of an A_4 singularity in these short-ranged attractive colloids.

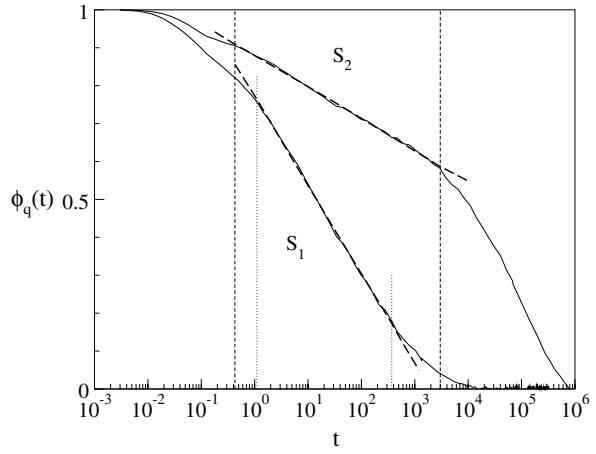

Figure 9. The density correlators for the binary SW system in the vicinity of the A_4 singularity for $\phi = 0.6075$ and $T = 0.4$. The two curves correspond to $\epsilon = 0.03$ (S_1) and 0.0411 (S_2). The vertical lines mark the regions of logarithmic behaviour and show the larger range of the S_2 case compared to the S_1 case.

3.4. The glass–glass line

The last MCT prediction that we want to test is the existence of a kinetic glass–glass transition. This is quite a difficult task, both experimentally and numerically, since there is obviously a need to access the glassy region, i.e. out-of-equilibrium states. To overcome this problem, we have adopted the following strategy. We started from an equilibrated configuration in the re-entrant liquid region, precisely at $\phi = 0.612$ and $k_BT/u_0 = 0.6$, and compressed it slowly to relevant packing fractions for the glass–glass transition. The value of the relative well width is 3%, i.e. the typical one for having a glass–glass transition in a SW system. Through the mapping described above, we estimated the glass–glass line to be located between (0.625, 0.37) and (0.64, 0.41) in the $(\phi, k_BT/u_0)$ plane. We focused on the isochore $\phi = 0.635$. Results for a different isochore and for a different initial state point were also presented [41], and shown to be qualitatively similar. Thus, the results shown here are independent of these particular choices. To study the dynamics along the glass–glass transition, we quenched our initial compressed configurations to various different final temperatures, both in the repulsive and in the attractive region, and looked at the behaviour of the density autocorrelation functions. If the transition exists, these should present clear distinct behaviours in the two regions, i.e. the repulsive one decaying to the typical hard sphere plateau and the attractive one relaxing only to the much higher plateau set by the attractive well width. However, there is a further issue to take into account, i.e. the role of the waiting time. To be sure that our results do not show dependence on ageing, we focused on studying a fairly definite time interval of about 400 MD units, after a waiting time $t_w \simeq 4000$. This choice ensures that in this limited, though narrow, time window, there are no ageing effects in the density correlators [20].

Having fully established the procedure, we show in figure 10 the results for the density correlators. What we observe in the top panel is not a clear separation, as expected from MCT predictions, between correlators in the attractive and in the repulsive glass, i.e. for temperatures below and above 0.4. For high temperatures within the repulsive glass region, the system, already in this small time window, is able to relax to the appropriate plateau, while for low temperatures in the attractive region, the expected high plateau is much less stable. Its duration

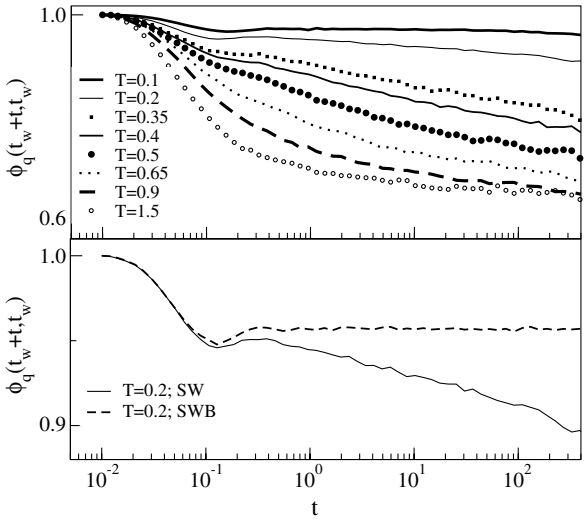

Figure 10. The density correlators for the binary SW system across the glass–glass line for $\phi = 0.635$ showing the effect of formation and breaking of bonds between particles.

only increases with decrease of the temperature, signalling that it is strongly connected to the bond dynamics taking place in the system. In other words, at finite temperatures the system has a finite probability of overcoming the energy barrier necessary to break a bond (in this model unambiguously defined by two particles at a distance smaller than the attractive well). The breaking and reforming of the bonds can be interpreted as the relevant 'hopping' processes for such systems, which have no effect on the repulsive glass for which bonds do not play a role, but do have a destabilizing effect for attractive glasses.

To support this conjecture, we compare in the bottom panel of figure 10 the dynamics of the square well system with that in a model where we artificially prevent any bond-breaking (and reforming) process. This model, consisting of a square well plus an infinitely thin barrier of height u_b (SWB), was introduced in [20, 42] and studied extensively in [43], varying the height of the barrier and thus the bond lifetime. The same initial configurations are used for the two models, so at time $t = 0$ the bonding patterns are identical. By construction, only decorrelation processes which do not modify the bonding pattern are possible in the SWB model. Here, we only show the correlators for the small temperature $k_B T/u_0 = 0.2$, with $u_b = 100u_0$, where the SWB model does indeed show the expected stable attractive plateau whose value is consistent with the expected value for the attractive glass. In contrast, correlators for the SW model have already decayed below the plateau value at short times. These results suggest that ideal MCT, by neglecting the bond-breaking processes, predicts a stability window for the short-ranged attractive glass larger than that observed in the simulation. This result is analogous to the behaviour of molecular liquids, in the sense that the attractive glass line has to be considered not as a sharp transition but as a line of crossover between two regions. In the first one, the repulsive glass, MCT predictions are very good because here activated processes do not play any significant role. The second one, the attractive glass, is an activated dynamics region controlled by the bond dynamics, where ideal MCT applies in a limited time window. In other words, our results suggest that MCT attractive glasses do not incorporate activated bond-breaking processes, in the same way that hopping processes are not considered for molecular glass formers. As a consequence, activated processes pre-empt the possibility of fully observing the glass–glass transition phenomenon predicted by MCT.

4. Conclusion and outlook

It has by now become clear that attractive interactions in colloidal systems show a rich phenomenology and have given rise to many interesting developments. Among the problems that we already quoted we included possible applications to the case of protein crystallization and to the formation of gel phases at low volume fractions. From the fundamental point of view it is worth stressing the possibility of understanding the interplay between percolation and attractive glass transitions, and the related question of the formation of a gel at low volume fractions. In this respect, the simultaneous evaluation of thermodynamic and dynamic arrest lines is a particularly important piece of information. Other possible important research lines which are beginning to emerge are related to the possibility of devising models where the phase separation process is suppressed and the low density arrested states can be approached from equilibrium studies. The work by Puertas *et al* [21], that of Coniglio and co-workers [44] and our recent work on charged short-range attractive colloids [45] appear to suggest a particular mechanism of formation of a gel phase composed of clusters, i.e. a glassy cluster phase. The relation between the arrest line at low packing fraction and the attractive glass line needs to be better clarified.

Acknowledgments

We acknowledge useful discussions throughout the years with W Götze and thank S Buldyrev for providing us with his MD code. We acknowledge support from MIUR PRIN, FIRB and INFM PRA-GENFDT, and also from INFM Iniziative Calcolo Parallelo and the Research and Training Network of the Marie Curie Programme of the EU (Contract Number: MRTN-CT-2003-504712).

References

[1] Sciortino F 2002 *Nat. Mater. News Views* **1** 145
[2] Anderson V J and Lekkerkerker H N V 2002 *Nature* **416** 811
[3] Baxter R J 1968 *J. Chem. Phys.* **49** 2770
[4] Miller M and Frenkel D 2003 *Phys. Rev. Lett.* **90** 135702
[5] Götze W 1991 *Liquids, Freezing and Glass Transition* ed J P Hansen, D Levesque and J Zinn-Justin (Amsterdam: North-Holland) p 287
[6] Fabbian L *et al* 1999 *Phys. Rev.* E **59** R1347
Fabbian L *et al* 1999 *Phys. Rev.* E **60** 2430
[7] Bergenholtz J and Fuchs M 1999 *Phys. Rev.* E **59** 5706
[8] Mallamace F *et al* 2000 *Phys. Rev. Lett.* **84** 5431
[9] Pham K N *et al* 2002 *Science* **296** 104
[10] Eckert T and Bartsch E 2002 *Phys. Rev. Lett.* **89** 125701
[11] Chen W R *et al* 2002 *Phys. Rev.* E **66** 021403
Chen W R *et al* 2003 *Phys. Rev.* E **68** 041402
[12] Chen S H *et al* 2003 *Science* **300** 619
[13] Pham K N *et al* 2004 *Phys. Rev.* E **69** 011503
[14] Grandjean J and Mourchid A 2004 *Europhys. Lett.* **65** 712
[15] Dawson K A 2001 *Phys. Rev.* E **63** 011401
[16] Puertas A M *et al* 2002 *Phys. Rev. Lett.* **88** 098301
[17] Foffi G *et al* 2002 *Phys. Rev.* E **65** 031407
[18] Foffi G *et al* 2002 *Phys. Rev.* E **65** 050802
[19] Zaccarelli E 2002 *Phys. Rev.* E **66** 041402
[20] Zaccarelli E *et al* 2003 *Phys. Rev. Lett.* **91** 108301
[21] Puertas A M *et al* 2003 *Phys. Rev.* E **67** 031406
[22] Sciortino F *et al* 2003 *Phys. Rev. Lett.* **91** 268301

[23] Zaccarelli E *et al* 2004 *Preprint* cond-mat/0402254
[24] van Megen W and Underwood S M 1993 *Phys. Rev. Lett.* **70** 2766
van Megen W and Underwood S M 1994 *Phys. Rev.* E **49** 4206
[25] Verduin H and Dhont J K G 1995 *J. Colloid Interface Sci.* **172** 425
[26] Bartsch E *et al* 1997 *J. Chem. Phys.* **106** 3743
[27] Foffi G *et al* 2000 *J. Stat. Phys.* **100** 363
[28] Barrat J L *et al* 1989 *J. Phys.: Condens. Matter* **1** 7163
[29] Piazza R 2000 *Curr. Opin. Colloid Interface Sci.* **5** 38
[30] Mushol M and Rosenberg F 1995 *J. Chem. Phys.* **103** 10424
[31] Gast A P *et al* 1983 *J. Colloid Interface Sci.* **96** 251
[32] Zaccarelli E *et al* 2001 *Phys. Rev.* E **63** 031501
[33] Bengtzelius U *et al* 1984 *J. Phys. C: Solid State Phys.* **17** 5915
[34] Sjögren L 1991 *J. Phys.: Condens. Matter* **3** 5023
[35] Mason T G and Weitz D A 1995 *Phys. Rev. Lett.* **75** 2770
[36] Zaccarelli E *et al* 2003 *Preprint* cond-mat/0310765
[37] Kob W and Barrat J-L 1997 *Phys. Rev. Lett.* **78** 4581
[38] Parisi G 1997 *J. Phys. A: Math. Gen.* **30** 8523
[39] Foffi G *et al* 2004 *J. Chem. Phys.* **120** 8824
[40] Sperl M 2003 *Phys. Rev.* E **68** 031405
[41] Zaccarelli E *et al* 2004 *J. Phys.: Condens. Matter* submitted
[42] Zaccarelli E *et al* 2003 *J. Phys.: Condens. Matter* **16** S367
[43] Saika-Voivod I *et al* 2004 *Preprint* cond-mat/0403320
[44] Del Gado E *et al* 2003 *Preprint* cond-mat/0310776
[45] Sciortino F *et al* 2003 *Preprint* cond-mat/0312161